Journal of proteome research

Article

pubs.acs.org/jpr

Comprehensive Characterization of Minichromosome Maintenance Complex (MCM) Protein Interactions Using Affinity and Proximity Purifications Coupled to Mass Spectrometry

Marie-Line Dubois, Charlotte Bastin, Dominique Lévesque, and François-Michel Boisvert*

Department of Anatomy and Cell Biology, Université de Sherbrooke, 3201 Jean-Mignault, Sherbrooke, Québec J1E 4K8, Canada

Supporting Information

ABSTRACT: The extensive identification of protein−protein interactions under different conditions is an important challenge to understand the cellular functions of proteins. Here we use and compare different approaches including affinity purification and purification by proximity coupled to mass spectrometry to identify protein complexes. We explore the complete interactome of the minichromosome maintenance (MCM) complex by using both approaches for all of the different MCM proteins. Overall, our analysis identified unique and shared interaction partners and proteins enriched for distinct biological processes including DNA replication, DNA repair, and cell cycle regulation. Furthermore, we mapped the changes in protein interactions of the MCM complex in response to DNA damage, identifying a new role for this complex in DNA repair. In summary, we demonstrate the complementarity of these approaches for the characterization of protein interactions within the MCM complex.

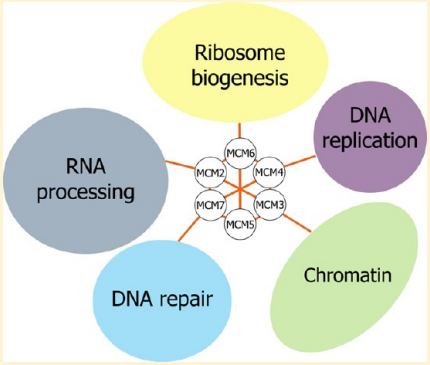

KEYWORDS: *MCM complex, DNA damage, DNA replication, mass spectrometry, SILAC, BioID, AP−MS*

INTRODUCTION

Traditional approaches using affinity purification followed by mass spectrometry identification of proteins (AP−MS) have been the mainstay for several years for studying protein−protein interactions.[1,2] This method relies on expressing a protein of interest fused to an epitope tag that facilitates affinity purification. Following cell lysis, antibodies or molecules conjugated to a solid support are used to isolate the protein of interest from a cell extract, along with interacting proteins. These proteins can then be identified by mass spectrometry, and experimental as well as bioinformatic quantitative methods can be applied to filter out contaminants and nonspecific protein interactions.[3−5] However, AP−MS relies on the solubility and the stability of the protein complexes and can thus bias the identification of interacting proteins.[6] Moreover, the presence of the epitope tag as well as overexpression of the bait protein can potentially interfere with protein interactions. An alternative approach that relies on proximity-dependent modification of neighboring proteins through biotinylation was recently introduced by Roux et al.[7] This method of purification by proximity coupled to mass spectrometry (PP−MS, also termed BioID), relies on the use of a nonspecific biotin protein ligase (BirA or APEX2) fused in frame with a protein of interest.[7,8] These enzymes produce a reactive biotin intermediate that quickly dissociate and react with proteins within a 20 nm radius.[9] Considering that BirA itself is ∼7.0 nm at its largest dimension,[10] we can expect biotinylation to occur up to three to four proteins around the protein of interest. Proteins interacting or in close proximity with the bait protein are thus found marked by this stable covalent modification, which can then be purified through more stringent, denaturing lysis conditions using streptavidin coupled to a solid support.[7,8]

During S phase, thousands of replication forks must be tightly regulated to make sure that DNA replication occurs only once.[11] The proteins involved in this process are recruited to origins of replications during the G1 phase of the cell cycle prior to initiation of DNA synthesis to prevent this duplicate replication of DNA,.[12] Once the DNA has been replicated, the proteins involved in replication can no longer be recruited, thus preventing each origin from being used twice during the S phase. This mechanism can be regulated by kinases involved in the DNA damage response (DDR), which can recognize stalled forks and inhibit the replication machinery from being activated, demonstrating a strong relationship between DNA replication and the cellular response to DNA damage.[13,14]

The sequential recruitment of the proteins involved in DNA replication is initiated by the loading of the MCM proteins with the proteins of the origin recognition complex (ORC), including Cdt6 and Cdt1.[15] The MCM complex contains six paralogs (MCM2 to MCM7) that form a ring structure and include a conserved domain, the AAA+ (ATPase associated with various cellular activities) found in several other DNA helicases.[16] MCM2−7 have been demonstrated to be required for both initiation and elongation of DNA replication,[17] and several overlapping mechanisms prevent the recruitment of more MCM

Received: November 27, 2015
Published: August 5, 2016

DOI: 10.1021/acs.jproteome.5b01081
J. Proteome Res. 2016, 15, 2924−2934

complexes onto origins of replication once DNA has been properly replicated during S phase.[18]

The MCM complex is thus central in determining the potential for DNA replication of cells. However, recent work demonstrated that the MCM proteins are not only regulated during the DNA replication phase but also interact directly with DNA repair proteins as well as proteins involved in cell cycle checkpoint control.[19,20] For example, the temperature-sensitive MCM yeast cells at restrictive temperature display an increase in phosphorylated histone H2A.x nuclear foci,[19] suggesting that a lack of functional MCM proteins results in an impaired DNA repair mechanisms. An interesting concept related to the MCM complex is the large excess of MCM proteins compared with the number required for each origin of replication. Indeed, in theory, only two DNA helicase complexes are necessary to start bidirectional DNA synthesis at the replication fork from each origin of replication. This "MCM paradox" refers to the idea that, in several different organisms including human cells, the amount of MCM proteins in the cells can be reduced by 90% without hindering DNA replication or cell cycle progression.[21−25] Additionally, most of the MCM proteins are not found at the sites of DNA synthesis, confirming a probable role for the MCM proteins in other cellular mechanisms. In addition, our recent study identified several proteins associated with MCM proteins following DNA damage, which demonstrated its potential role in chromatin remodeling and histone proteins deposition during mechanisms of DNA repair.[26]

In this study, we explored the combination of two protein complexes purification approaches to study proteins interacting with the MCM complex. To identify the complete MCM complex interactome, we generated cell lines stably expressing either GFP or BirA fusion proteins for each MCM proteins and applied a quantitative proteomic strategy using stable isotope labeling of amino acids in cell culture (SILAC). Our results using AP−MS and PP−MS for each of the MCM proteins demonstrate that the MCM complex becomes strongly associated with nuclear structures following exposure to DNA damage. We identified an intriguing array of interaction partners that includes not only the core MCM2−7 proteins but also several proteins involved in chromatin organization, DNA repair, and cell-cycle regulation. These results provide valuable clues pointing toward a role for the MCM complex not only during DNA replication but also during the cellular response to DNA damage.

■ MATERIALS AND METHODS

Antibodies

The antibodies used for immunoblotting and immunofluorescence experiments were: anti-GFP (Roche 11814460001), anti-GAPDH (Rabbit monoclonal, Cell Signaling no. 2118S), Streptavidin-HRP (Cell Signaling no. 3999), anti-MCM2 (Rabbit polyclonal, Abcam no. Ab31159), anti-MYC (hybridoma, ATCC, CRL-1729), anti-γH2AX (Rabbit polyclonal, Santa Cruz no. sc-101696), and anti-SF3B3 (Rabbit polyclonal, A302-508, Bethyl Laboratories). The following secondary antibodies were used: antimouse IgG-HRP (Goat polyclonal, Santa Cruz no. sc-2005) and antirabbit IgG-HRP (Goat polyclonal, Santa Cruz no. sc-2004).

Immunofluorescence Microscopy

Cells were grown on glass coverslips and fixed by the addition of 1% paraformaldehyde in PBS for 10 min. Following this incubation, cells were washed with PBS and incubated PBS containing 0.5% of Triton X-100 for 10 min, followed by washing in PBS. Coverslips were then inverted onto a solution containing the primary antibodies diluted in PBS for 1 h. The coverslips were then washed once with PBS containing 0.1% Triton X-100 and twice with PBS. The coverslips were then incubated with the secondary antibodies conjugated to either Alexa 488 or 546 (Molecular Probes) for 1 h in PBS. DNA was visualized with DAPI (4.6-diamidino-2-phenylindole), and the coverslips were mounted on glass slides with the antifading agent Shandon Immuno-Mount (Thermo Scientific).

Cloning and Generation of Plasmids

The cDNAs for the six different MCM proteins (MCM2 to MCM7) were obtained by PCR from a cDNA library generated by RT-PCR with an oligo-dT following isolation of mRNA on U2OS cells. The oligonucleotides included BP recombination sites for insertion by recombination into pDONR 221 (Life Technologies) using BP recombinase and were subsequently cloned into pgLAP1 (Addgene) using LR recombinase (Gateway cloning, Life Technologies). The pbLAP1 was obtained by removing GFP from pgLAP1 by PCR, and BirA* was synthesized by gBlocks Gene Fragments.

Cell Culture and Stable Cell Lines

The U2OS and U2OS Flp-In T-Rex cells were grown as adherent cells in Dulbecco's modified eagle medium (DMEM) supplemented with 10% fetal bovine serum. For culture in SILAC media, DMEM depleted of arginine and lysine (Life Technologies A14431-01) was supplemented with 10% dialyzed fetal bovine serum (Invitrogen, 26400-044), 100 U/mL penicillin/streptomycin, and 2 mM GlutaMax. Arginine and lysine were added in either light (Arg0, Sigma, A5006; Lys0, Sigma, L5501), medium (Arg6, Cambridge Isotope Lab (CIL), CNM-2265; Lys4, CIL, DLM-2640), or heavy (Arg10, CIL, CNLM-539; Lys8, CIL, CNLM-291) to a final concentration of 28 μg/mL of arginine and 49 μg/mL of lysine. To prevent proline to arginine conversion, we added a final concentration of 10 μg/mL of L-proline.

Stable cell lines expressing either GFP or BirA* were generated by transfecting either the pgLAP1 or pbLAP1 (see Cloning and Generation of Plasmids section) along with the Flp-recombinase encoded by the plasmid pOG44. The selection was performed by adding 150 μg/mL Hygromycin B and 15 ug/mL Blasticidin-HCl to the culture. The proteins were induced with 2 μg/mL Doxycyclin for 48 h, and the biotinylation for the BirA-tagged proteins was produced by adding 50 μM biotin for 24 h. The topoisomerase II inhibitor etoposide (#E1383, Sigma-Aldrich) was used for the induction of DNA damage.

GFP-Immunoprecipitation from SILAC-Labeled Cells

Cells were harvested separately by scraping in PBS, and the pellets were lysed in high-salt buffer (1% NP-40, 50 mM Tris ph7.5, 300 mM NaCl, 150 mM KCl, 5 mM EDTA, 1 mM DTT, 10 mM NaF, 10% glycerol, Roche Complete Protease Inhibitor Cocktail) for 10 min on ice. Insoluble material was pelleted by centrifugation for 10 min at 13 000g at 4 °C, and the supernatants from the three SILAC conditions were combined. The immunoprecipitation was performed by adding GFP-Trap agarose beads from ChromaTek (Martinsried, Germany) for 2 h at 4 °C. The beads were then washed with high-salt buffer and finally with PBS. The beads were then suspended in loading sample buffer and separated by SDS-PAGE and the samples processed as follows.

Gel Electrophoresis and In-Gel Digestion

The immunoprecipitated proteins were reduced with 10 mM DTT and alkylated with 50 mM iodoacetamide incubated at 95 °C for 5 min in 1× Laemmli buffer and then separated by

DOI: 10.1021/acs.jproteome.5b01081
J. Proteome Res. 2016, 15, 2924−2934

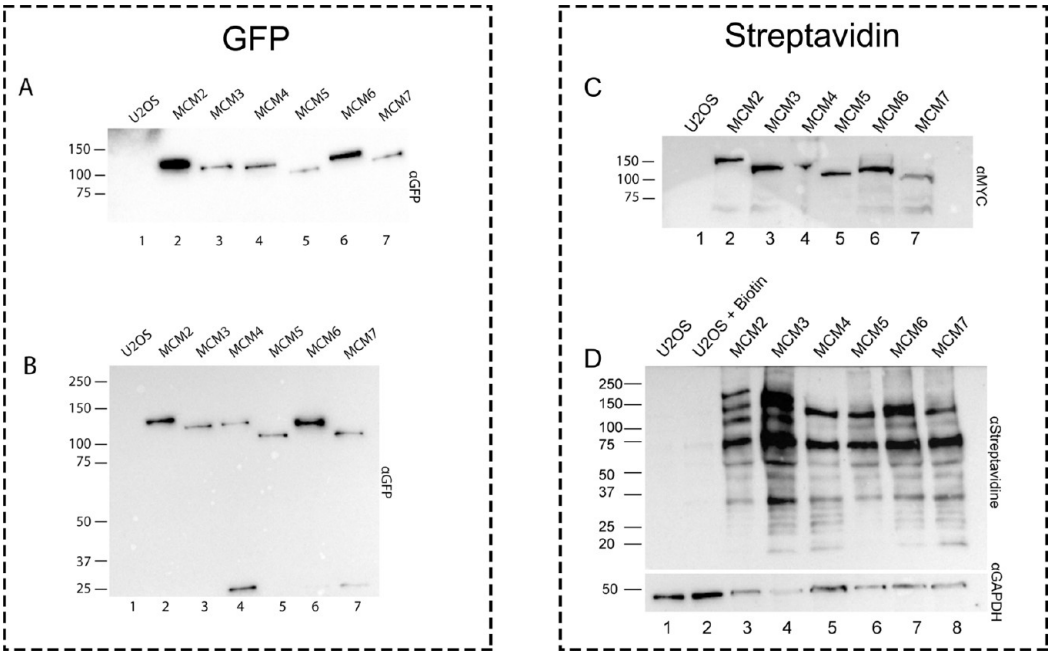

Figure 1. (A) Total protein lysates from U2OS cells stably expressing each of the GFP-tagged MCM proteins were analyzed by Western blotting using a GFP antibody. (B) Immunoprecipitates using GFP-Trap beads of each cell line stably expressing GFP-tagged MCM proteins were analyzed by Western blotting using a GFP antibody. (C) Protein lysates from U2OS cells expressing each of the mycBirA tagged MCM proteins were analyzed by Western blotting using a myc antibody. (D) Protein lysates from U2OS cells expressing each of the mycBirA tagged MCM proteins were analyzed using streptavidin coupled to HRP.

SDS-PAGE gel electrophoresis (4−12% Bis-Tris Novex mini-gel, Life Technologies). The gel was washed and stained with Coomassie Blue (Simply Blue Safe Stain, Life Technologies). Following extensive washes in water, the gel was cut into slices with a clean scalpel, destained, and digested with trypsin (Trypsin Gold, mass-spectrometry grade, Promega Corporation, Fitchburg, WI). The peptides were then extracted by adding 1% formic acid, then 100% acetonitrile. The solvent was removed by lyophilization in a speed vacuum centrifuge, and the tryptic peptides were resuspended in 1% formic acid.

Streptavidin Purification from SILAC-Labeled Cells

U2OS cells grown in each SILAC medium were harvested separately by scraping in PBS, and the cell pellets were lysed in high salt buffer (1% NP-40, 50 mM Tris ph7.5, 300 mM NaCl, 150 mM KCl, 5 mM EDTA, 1 mM DTT, 10 mM NaF, 10% glycerol, Roche Complete Protease Inhibitor Cocktail) for 10 min on ice. The lysates were then sonicated three times for 5 s and centrifugated for 10 min at 13 000*g* at 4 °C. The lysates from the three SILAC conditions were combined, and proteins labeled from each SILAC medium were incubated with streptavidin high-performance beads (GE Healthcare) for 2 h at 4 °C. Following the incubation, the beads were washed three times with high-salt buffer and five times with 20 mM NH_4HCO. The samples were processed for on-bead digestion.

On-Beads Digestion

For each immunoprecipitation, proteins on beads were reduced with 10 mM DTT, boiled, and alkylated with 15 mM iodoacetamide. The proteins were digested overnight with trypsin (Trypsin Gold, mass-spectrometry-grade, Promega Corporation). The resulting tryptic peptides were extracted by 1% formic acid and then 60% CH_3CN/0.1% formic acid. The solvent was removed by lyophilization in a speed vacuum centrifuge and resuspended in 1% formic acid.

LC−MS/MS

The peptides from each separate experiments were loaded onto a Dionex Ultimate 3000 nanoHPLC system. Ten μL of the sample (~2 μg) resuspended in 1% (v/v) formic acid was loaded with a constant flow of 4 μL/min onto a trap column (Acclaim PepMap100 C18 column (0.3 mm id × 5 mm, Thermo Scientific)). The peptides were then eluted off and loaded onto a PepMap C18 nano column (75 μm × 50 cm, Thermo Scientific) with a linear gradient of 5−35% solvent B (90% acetonitrile with 0.1% formic acid) over a 4 h gradient with a constant flow of 200 nL/min. The peptides were then electrosprayed into an OrbiTrap QExactive mass spectrometer (Thermo Scientific) by an EasySpray source. The spray voltage was 2.0 kV and the temperature of the analytical column was at 40 °C. The acquisition of the full-scan MS survey spectra (m/z 350−1600) in profile mode was performed in the Orbitrap at a resolution of 70 000 using 1 000 000 ions. The peptides selected for fragmentation by collision-induced dissociation were based on the ten highest intensities for the peptide ions from the preview scan. The normalized collision energy was set at 35%, and the resolution was set at 17 500 for 50 000 ions. The filling times was set to a maximum of 250 ms for the full scans and 60 ms for the MS/MS scans. All unassigned charge states as well as singly, seven, and eight charged species for the precursor ions were rejected. Additionally, a dynamic exclusion list was set to retain up to 500 entries with a maximum retention time of 40 s using a 10 ppm mass window. To improve the mass accuracy of survey scans, we enabled the lock mass option. Data acquisition was done using Xcalibur version 2.2 SP1.48.

Quantification and Bioinformatics Analysis

Protein identification and quantification was performed using the MaxQuant software package version 1.4.1.2 as previously described[27] with the protein database from Uniprot (*Homo sapiens*, 16/07/2013, 88 354 entries). For protein identification,

DOI: 10.1021/acs.jproteome.5b01081
J. Proteome Res. 2016, 15, 2924−2934

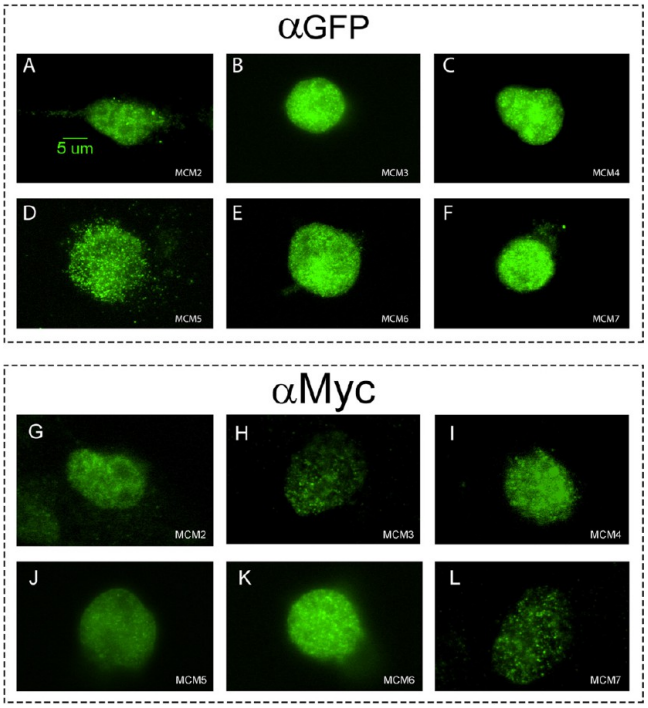

Figure 2. Representative immunofluorescence images of U2OS cells stably expressing either GFP-tagged MCM 2−7 (A−F) or mycBirA-tagged MCM2−7 (G−L).

carbamidomethylation on cysteine was used as a fixed modification, and methionine oxidation and protein N-terminal acetylation were used as variable modifications. The enzyme was set to trypsin, with no cleavages on lysines or arginines before a proline, and up to two miscleavages were allowed. The mass tolerance was set at a maximum of 7 ppm for the precursor ions and 20 ppm for the fragment ions. Requantification of selected isotopic patterns was allowed to obtain ratios of all SILAC pairs.[28] We set a threshold of 1% for the false discovery rate (FDR) based on the criteria that the number of forward hits identified from the database was at least 100 times higher than the number proteins identified in a database containing reverse protein sequences. For protein quantification, we set the a minimum of two peptides identified for each protein. The mass spectrometry data have been deposited to the ProteomeXchange Consortium (http://proteomecentral.proteomexchange.org) via the PRIDE partner repository with the data set identifier PXD004089.

■ RESULTS

Generation of Cell Lines Stably Expressing GFP-MCM2−7 or mycBirA-MCM2−7

Our previous study using AP−MS of GFP-MCM2 has identified several proteins involved in DNA replication as well as some proteins whose interaction was increased following DNA damage.[26] These findings encouraged us to study further the

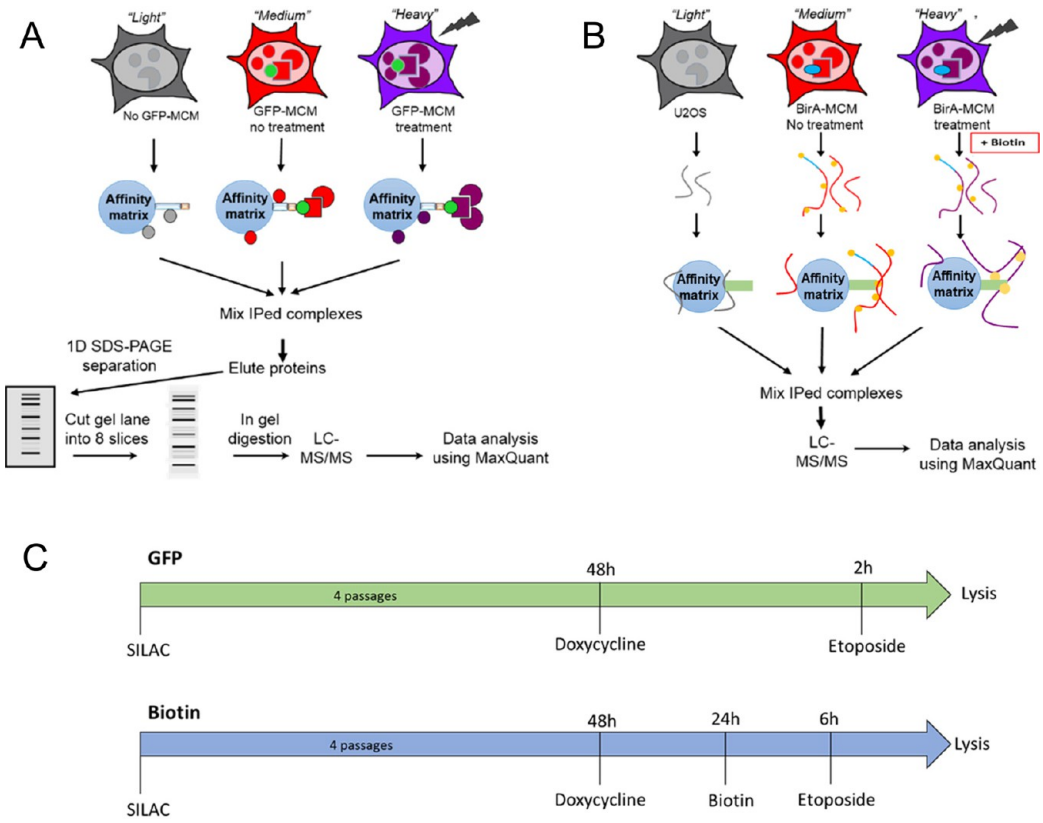

Figure 3. Experimental scheme for quantitative SILAC IP identification of MCM proteins using either GFP pulldowns (AP−MS, (A)) or biotin pulldowns (PP−MS, (B)). Cells not expressing any tagged proteins were grown in light, normal containing isotopes medium as control and compared with either cells expressing the tagged proteins (medium SILAC media) or cells expressing the tagged proteins treated with etoposide to induced DNA damage (heavy SILAC media). The immunoprecipitates were combined prior to separation by SDS page for AP−MS an in-gel trypsin digestion or directly digested on-beads for streptavidin pulldowns. (C) Schematic of the timeline of induction of expression of the tagged proteins by doxycycline, the addition of the biotin substrate for BirA, and induction of DNA damage by etoposide prior to cell lysis.

DOI: 10.1021/acs.jproteome.5b01081
J. Proteome Res. 2016, 15, 2924−2934

MCM complex to identify and characterize all of the interactions under normal growth condition as well as following DNA damage.

To gain further insight into a complete map of protein interactions with the MCM complex, we generated cell lines stably expressing each of the MCM proteins, either with a GFP tag for AP−MS (Figure 1A) or with a BirA tag for PP−MS experiments (Figure 1C). We have used U2OS human osteosarcoma cells using an Flp-In T-Rex system to ensure a known integration site as well as regulated expression under the control of a tetracycline repressor. The U2OS parental cells were used as controls. Immunoprecipitation using GFP-TRAP agarose beads has been shown to be highly efficient for the purification of protein complexes with very little interference or nonspecific binding.[1,29] Analysis of protein levels in their respective stable cell lines confirmed the expression of proteins of the expected molecular weight (Figure 1A,C). Immunoprecipitation using GFP-TRAP confirmed the isolation of the GFP-tagged proteins (Figure 1B), and incubation of cells with the biotin substrate for BirA resulted in specific biotinylation of proteins, as visualized by streptavidin-HRP of whole cell lysates (Figure 1D). Furthermore, subcellular localization of the GFP- (Figure 2A−F) and BirA- (Figure 2G−L) tagged MCM proteins is consistent with endogenous localization showing a predominantly nuclear staining by immunofluorescence. These observations show that our stable cell lines express each of the MCM proteins with proper molecular weight and subcellular localization, indicating that the GFP or BirA tag does not interfere with protein stability or subcellular localization.

Affinity Purification and Proximity Purification of Protein Complexes Followed by Quantitative Mass-Spectrometry Identification

Next, we investigated protein interactions by performing a triple-labeling SILAC-based proteomics identification and quantitation of interaction partners using both methods (Figure 3). This quantitative approach allows us to differentiate specific interactions from contaminant or abundant proteins. Cells not expressing the protein of interest were grown in "light" (L) media and used as a control for nonspecific binding. To identify proteins specifically interacting with our protein of interest (Figure 3A), or in proximity to our protein of interest (Figure 3B), cells were grown in "medium" (M) media prior to lysis and purification. To quantify changes in interaction following DNA damage, cells grown in "heavy" (H) media were treated with etoposide, a topoisomerase II inhibitor causing protein−DNA adducts resulting in double-stranded DNA breaks for either 2 h prior to lysis for GFP immunoprecipitations or 6 h prior to lysis for biotinylation (Figure 3C). The time of treatment for DNA damage in the PP−MS experiment was increased because the biotinylation reaction is much slower and biotin is typically incubated for a total of 24 h. To find a compromise between the response to DNA damage and the time required for biotinylation, we incubated the cells expressing BirA tagged proteins with biotin for a total of 24 h and induced DNA damage by the addition of etoposide in the last 6 h of the reaction, when the BirA-tagged protein is expressed at its highest. Cells were cultured in the SILAC media for at least five passages to confirm the incorporation

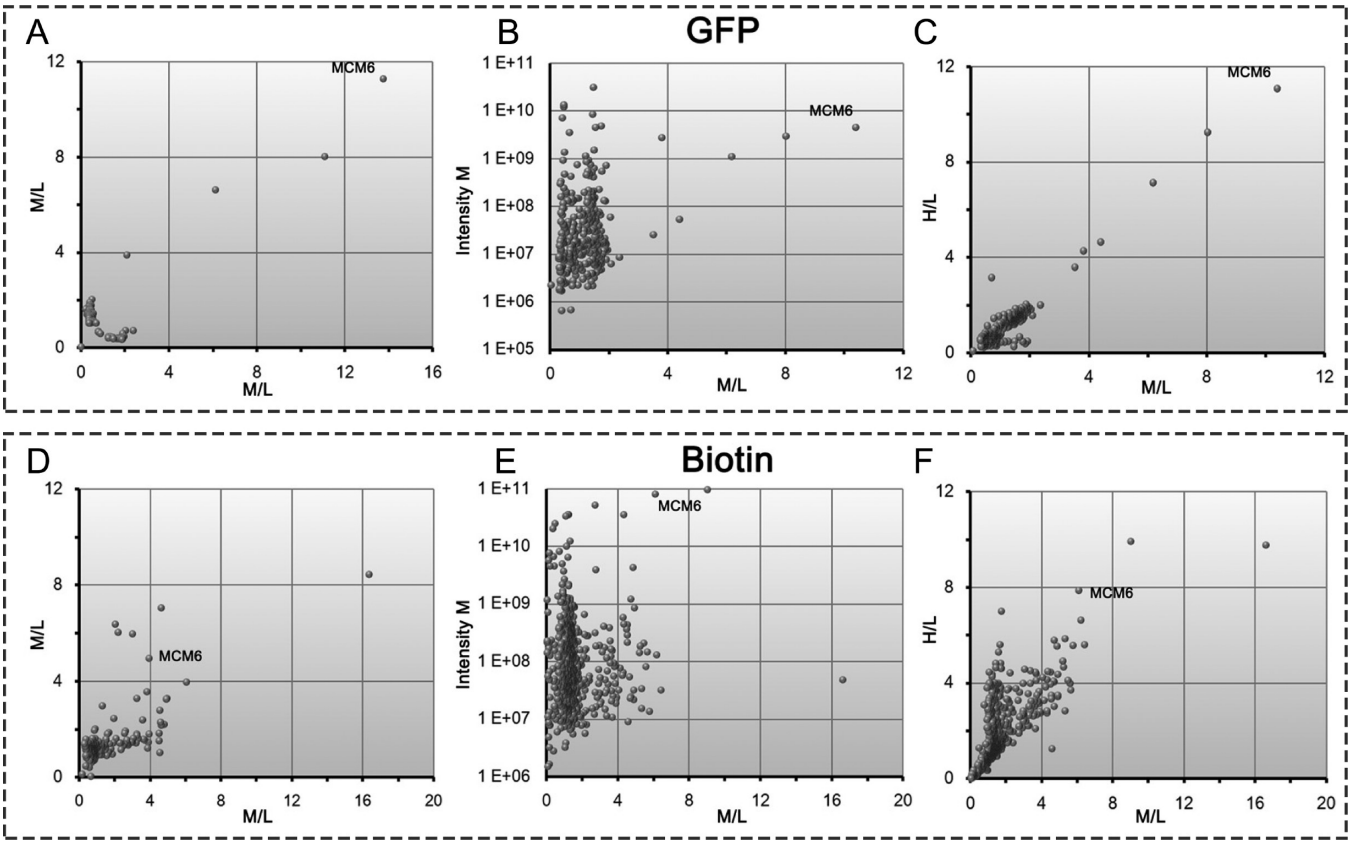

Figure 4. Scatter plot of the $\log_2$ SILAC ratios for proteins identified with MCM6 by AP−MS (A,C,E) and PP−MS (B,D,F). Two repeats of the experiments are compared for (A) AP−MS and (B) PP−MS with the M/L ratios for each experiment. The average $\log_{10}$ of both experiments of the intensities is plotted against the average M/L ratios for (C) AP−MS and (D) PP−MS. Average $\log_2$ SILAC ratios of etoposide-treated cells (H/L) over nontreated cells (M/L) for (E) AP−MS and (F) PP−MS. All other MCM proteins scatter plots can be found in the Supplementary Tables.

DOI: 10.1021/acs.jproteome.5b01081
J. Proteome Res. 2016, 15, 2924−2934

of each isotopic amino acids, and each experiment was repeated twice.

Following lysis, total cell lysates are mixed and subjected to either immunoprecipitation using the high-affinity GFP-Trap_A reagent (Figure 3A) or to purification using streptavidin-agarose (Figure 3B). For the GFP immunoprecipitations, the eluted proteins were resolved by 1D SDS-PAGE, and the coomassie-stained gel was separated into eight slices for in-gel digestion and mass spectrometry analysis (Figure 3A). The identified proteins by AP−MS for the six MCM proteins are provided in Supplementary Table 1. For the streptavidin pulldowns of biotinylated proteins, it proved difficult to elute the proteins from the agarose beads, and we thus performed trypsin digestion directly on the beads and eluted the digested peptides for MS analysis (Figure 3B). The identified proteins by PP−MS for the six MCM proteins are provided in Supplementary Table 2.

Protein Identification Using AP−MS versus PP−MS and Proteomic Analysis

According to the mass differences arising from the differentially labeled peptides detected, the different M/L, H/L, and H/M ratios are measured for each protein identified. These ratios represent if the proteins were specifically enriched (M/L and H/L) and whether the protein enrichment changed following treatment with etoposide (H/M). To illustrate an example of the results obtained with one of the MCM proteins, the distribution of the SILAC ratios of two biological repeat experiments is shown for MCM6 in Figure 4. Only proteins found in both repeats of the experiments with M/L ratios above two are considered as specific interactors (Figure 4A,D). As expected, most of the proteins identified bind nonspecifically to the agarose beads and are discarded in further analysis. It is also possible to compare the ratio of enrichment M/L with the average intensities of the peptides identified for a protein to provide an estimate in the amount of proteins present, reflecting the stoichiometry of the interaction (Figure 4B,E). In all cases, the purified protein has the highest intensity along with the tag (GFP or BirA). Finally, the representation of M/L versus H/L ratios allows visualizing changes in protein interactions following DNA damage (Figure 4C,F). Proteins near the line with a slope = 1 (H/M = 1) indicate no changes in interactions, whereas proteins with a higher H/L ratio indicate an increase in protein interactions with the immunoprecipitated protein, whereas proteins with a lower H/L ratios indicate a decrease in proteins interactions following DNA damage.

Identification of Proteins Interacting with the MCM Complex: An Overview

To identify proteins that were consistently enriched with the MCM complex using both AP−MS and PP−MS approaches, we compared the overlap between the two methods, and the results are displayed as a Venn diagram (Figure 5A,B). Proteins with a ratio M/L above two that were identified interacting with at least two different MCM proteins were kept for both the AP−MS and the PP−MS experiments. The list of proteins is available in Supplementary Table 3. In total, we identified 117 proteins interacting with the MCM complex using GFP immunoprecipitations (Figure 5, green) and 125 proteins interacting with the MCM complex using streptavidin pulldowns of biotinylated proteins (Figure 5, red). To discriminate between unreported and known interactions for the MCM complex, we compared the proteins identified in our AP and PP−MS experiments with IntAct, a database of curated interactions from published literature or from direct data deposition.[30] We limited the database to

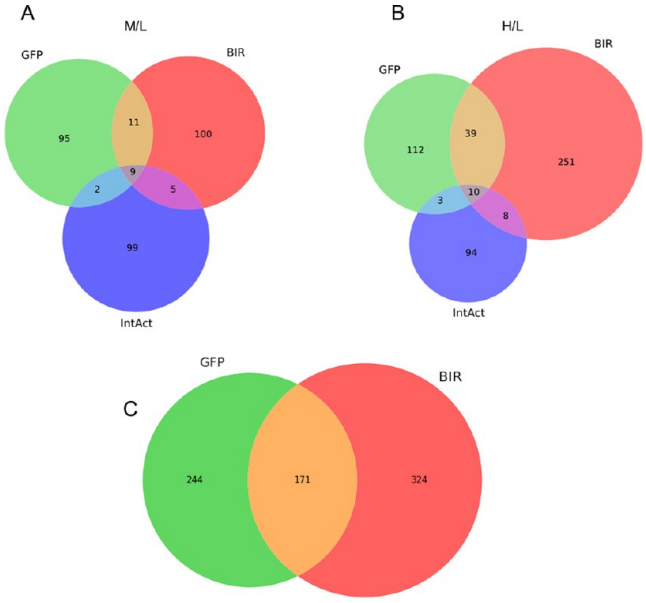

Figure 5. Overlap between the AP−MS, PP−MS and interactions from IntAct are displayed as a Venn diagram (A) without treatment or (B) following treatment with Etoposide. Proteins with a ratio M/L above two that were identified interacting with at least two different MCM proteins were kept for both the AP−MS and the PP−MS experiments. In total, 117 proteins interacting with the MCM complex using GFP immunoprecipitations (A) and 125 proteins interacting with the MCM complex using streptavidin pulldowns of biotinylated proteins (B) are shown. IntAct is a database of curated interactions from published literature or from direct data deposition. The database was limited to human interactions, and interactions from large screens were selected when identified in at least two separate studies. The number of known interactions in IntAct for all of the proteins of the MCM complex was 115 (blue). (C) Overlap when considering all proteins identified with the AP−MS or PP−MS is much greater.

human interactions and kept interactions from large screens (such as yeast two-hybrids) when they were confirmed in at least two separate studies. The number of known interactions in IntAct for all proteins of the MCM complex was 115 (Figure 5, blue). When comparing all of these interactions, the six proteins of the MCM complex were identified as interacting with each other using the three approaches, as expected (Figure 5A, the overlap of the three circles), indicating that each of the MCM proteins expressed does assemble into a complete MCM complex. An additional 10 interactions identified in our experiments have already been characterized, confirming that our method has identified known protein interactions (Figure 5A, overlaps with either blue and green or blue and red). Interestingly, 11 proteins identified in both our experiments (Figure 5A, the overlap of green and red circles) have not been described before, along with a large number of potential interactions that were identified with either method alone. However, if we consider proteins interacting with only one of the MCM proteins from each experiment, the overlap between the two methods is much greater and we identified 171 proteins interacting with the MCM protein in both experiments (Figure 5C).

Following DNA damage, we identified 49 proteins interacting with the MCM complex using both AP−MS and PP−MS (Figure 5B, overlap between green and red), up from 20 in the absence of DNA damage. To identify the function of the proteins identified, we analyze the gene ontology annotations enrichment for biological processes using DAVID.[31,32] Proteins identified

DOI: 10.1021/acs.jproteome.5b01081
J. Proteome Res. 2016, 15, 2924−2934

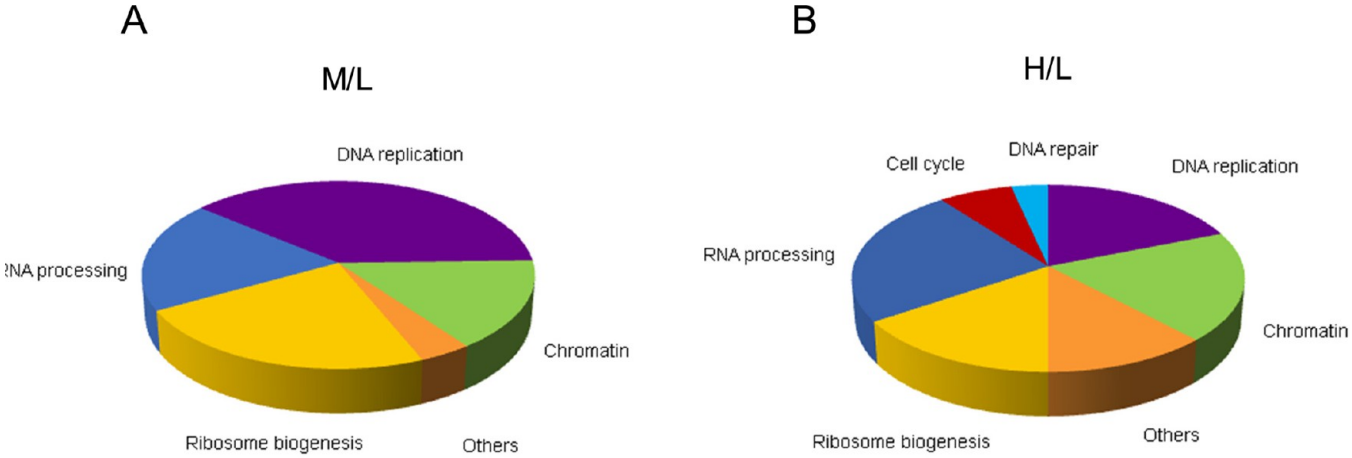

C

DNA replication	Gene Name	Protein Name
Q13416	ORC2	Origin recognition complex subunit 2
Q13415	ORC1	Origin recognition complex subunit 1
Q9UBD5	ORC3	Origin recognition complex subunit 3
O43913	ORC5	Origin recognition complex subunit 5
P33991	MCM4	DNA replication licensing factor MCM4
P25205	MCM3	DNA replication licensing factor MCM3
P33992	MCM5	DNA replication licensing factor MCM5
P33993	MCM7	DNA replication licensing factor MCM7
P49736	MCM2	DNA replication licensing factor MCM2
Q14566	MCM6	DNA replication licensing factor MCM6
Q9BTE3	MCMBP	MCM complex-binding protein

Ribosome biogenesis	Gene Name	Protein Name
Q9Y3U8	RPL36	60S ribosomal protein L36
Q9Y2P8	RCL1	RNA 3'-terminal phosphate cyclase-like protein
Q9BVJ6	UTP14A	3 small nucleolar RNA-associated protein 14 homolog A
Q9NYH9	UTP6	J3 small nucleolar RNA-associated protein 6 homolog
P62241	RPS8	40S ribosomal protein S8
Q9Y2X3	NOP58	Nucleolar protein 58
Q9Y5J1	UTP18	I3 small nucleolar RNA-associated protein 18 homolog
P56537	EIF6	Eukaryotic translation initiation factor 6
Q9NV31	IMP3	U3 small nucleollar ribonucleoprotein protein IMP3
F8W181	RPL6E	60S Ribosomal Protein L6e
J3QSV6	RSL1D1	Ribosomal L1 domain-containing protein 1

Others	Gene Name	Protein Name
Q9H0H5	RACGAP1	Rac GTPase-activating protein 1
A2A2D0	STMN1	Stathmin
P37802	TAGLN2	Transgelin-2
Q15061	WDR43	WD repeat-containing protein 43
P31431	SDC4	Syndecan-4
Q14192	FHL2	Four and a half LIM domains protein 2
P63104	YWHAZ	14-3-3 protein zeta/delta

Chromatin	Gene Name	Protein Name
O75531	BANF1	Barrier-to-autointegration factor
Q99880	HIST1H2BL	Histone H2B type 1-L
O75367	H2AFY	Core histone macro-H2A.1
Q16778	HIST2H2BE	Histone H2B type 2-E
Q71UI9	H2AFV	Histone H2A.V
Q14683	SMC1A	Structural maintenance of chromosomes protein 1A
Q9UQE7	SMC3	Structural maintenance of chromosomes protein 3
Q99878	HIST1H2AJ	Histone H2A type 1-J
Q08945	SSRP1	FACT complex subunit SSRP1
P62805	HIST1H4A	Histone H4

RNA processing	Gene Name	Protein Name
O75533	SF3B1	Splicing factor 3B subunit 1
Q9NVP1	DDX18	ATP-dependent RNA helicase DDX18
P38919	EIF4A3	Eukaryotic initiation factor 4A-III
P62316	SNRPD2	Small nuclear ribonucleoprotein Sm D2
Q96GQ7	DDX27	Probable ATP-dependent RNA helicase DDX27
P08579	SNRPB2	U2 small nuclear ribonucleoprotein B''
Q15459	SF3A1	Splicing factor 3A subunit 1
P11940	PABPC1	Polyadenylate-binding protein 1
P09661	SNRNPA1	U2 small nuclear ribonucleoprotein A'
P55769	SNU13	NHP2-like protein 1
Q9BXY0	MAK16	Protein MAK16 homolog
Q13435	SF3B2	Splicing factor 3B subunit 2
Q9Y5S9	RBM8A	RNA-binding protein 8A

Cell cycle	Gene Name	Protein Name
Q6PL18	ATAD2	ATPase family AAA domain-containing protein 2
Q96C19	EFHD2	EF-hand domain-containing protein D2
P46087	NOP2	Probable 28S rRNA (cytosine(4447)-C(5))-methyltransferase

DNA repair	Gene Name	Protein Name
P11388	TOP2A	DNA topoisomerase 2-alpha
O75569	PRKRA	:erferon-inducible dsRNA-dependent protein kinase activator

Figure 6. Proteins interacting with the MCM complex using both AP−MS and PP−MS (Figure 5, the overlap between green and red) were analyzed for gene ontology annotations enrichment for biological processes using DAVID (A) in the absence of treatment or (B) following treatment with Etoposide.

interacting with the MCM complex included four different biological processes (Figure 6A and Supplementary Table 4). The main process identified included proteins involved in DNA replication as well as chromatin remodeling, consistent with the known role for the MCM complex as a DNA helicase involved in DNA replication. Moreover, we identified several proteins involved in either ribosome biogenesis or RNA processing. Interestingly, following DNA damage, we identified the same four biological process annotations but also identified proteins involved in DNA repair and cell cycle regulation (Figure 6B), indicating that some of the proteins interacting with MCM proteins following the treatment with Etoposide are involved in these processes.

To further illustrate individually the proteins involved, we established an interaction map based on the proteins identified by AP−MS and PP−MS (Figure 7, nodes) and compared with known interactions (Figure 7, lines). The proteins that we identified were grouped according to the biological processes identified in Figure 6 (Figure 7, large circles), with the MCM proteins in the middle. Proteins not involved in these biological processes were separated on the outside (Figure 7, others), and the known interactions are displayed when appropriate. As expected, all MCM proteins are well-characterized to interact with each other, as exemplified by the numerous lines between them. Additionally, several known interactions with proteins involved in DNA replication such as proteins involved

DOI: 10.1021/acs.jproteome.5b01081
J. Proteome Res. 2016, 15, 2924−2934

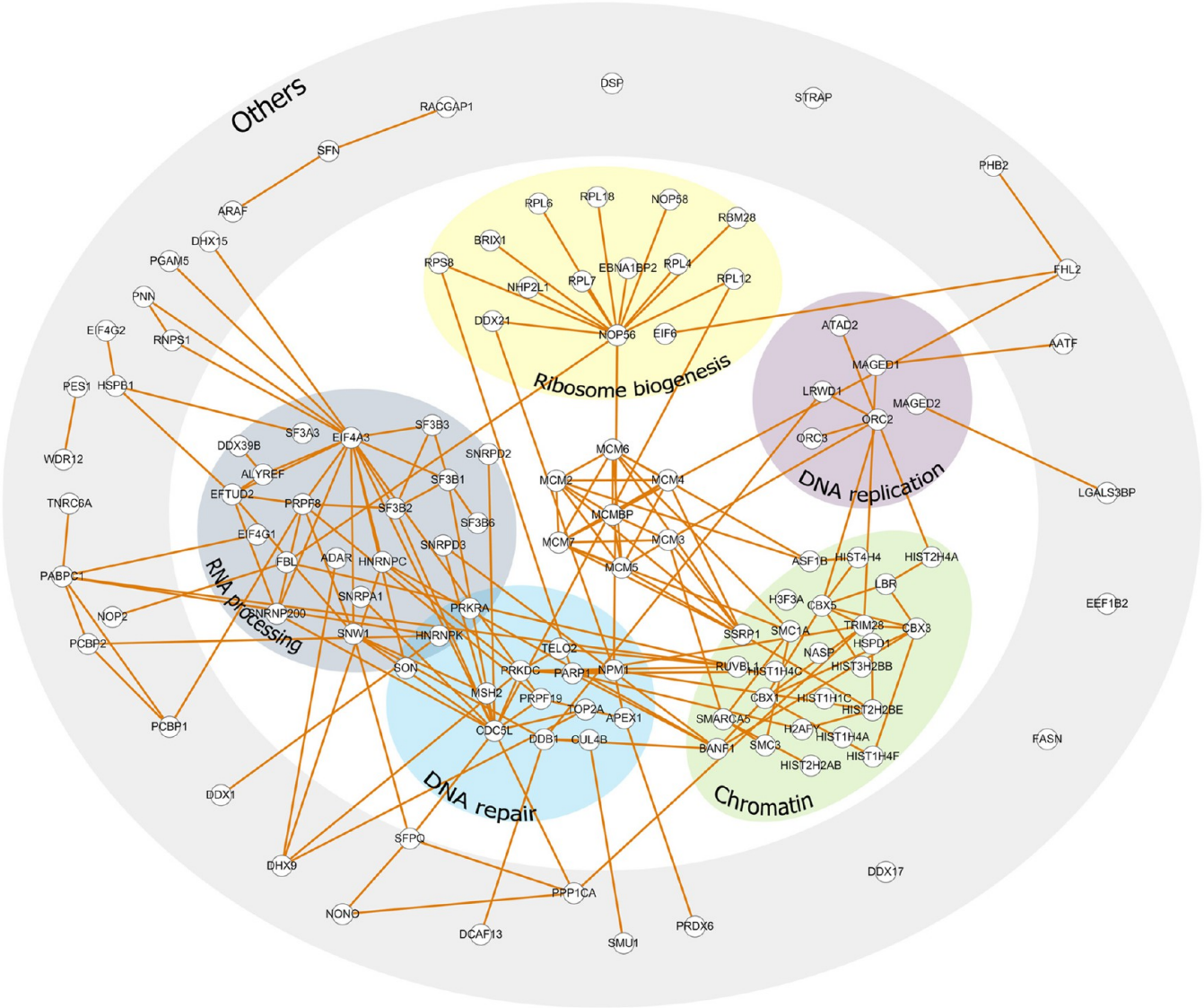

Figure 7. Interaction map based on the proteins identified by AP−MS and PP−MS (nodes) are compared with known interactions (lines). The proteins that were identified were grouped according to the biological processes identified in Figure 6 (large circles), with the MCM proteins in the middle. Proteins not involved in these biological processes were separated on the outside (others), and the known interactions are displayed when appropriate.

in the recognition of the origins of replication (ORCs) were identified. The group of proteins with the largest number of previously reported interaction consisted of proteins involved in chromatin remodeling. Interestingly, several proteins involved in ribosome biogenesis and RNA processing were identified, and even though there is not much known regarding a potential role for the MCM complex in these processes, it is rather intriguing that the proteins identified do not appear to be random proteins involved in these processes but are actually proteins known to be part of the same complexes with defined functions.

To validate the results obtained in the interaction studies, we performed coimmunoprecipitations followed by immunoblotting to confirm the interaction between some of the proteins that were identified (Figure 8). Immunoprecipitation of GFP-DDB1 revealed an interaction with MCM2 that increased following treatment with Etoposide (Figure 8B). Similarly, the interaction between GFP-MCM7 and one of the splicing factor (SF3B3) that was identified was also confirmed (Figure 8D), and this interaction also increased following DNA damage.

■ DISCUSSION

In this study, we explored the combination of two protein complexes purification approaches to study proteins interacting with the MCM complex. We generated cell lines stably expressing either GFP or BirA fusion proteins for each MCM proteins and applied a quantitative proteomic strategy using stable isotope labeling of amino acids in cell culture (SILAC). This provides for the first time a very complete and thorough study of all protein interactions with the MCM complex. Our results using AP−MS and PP−MS for each of the MCM proteins demonstrate that the MCM complex becomes associated with proteins including the core MCM2−7 proteins and also several proteins involved in chromatin organization, DNA repair, and cell cycle regulation. The results from this extensive characterization of protein interactions provide valuable clues pointing toward a role for the MCM complex in chromatin remodeling following cellular exposure to DNA damage (Figure 6 and Supplementary Table 5).

While this study identified a large number of putative protein interactions, we restricted our follow-up analyses using only the

DOI: 10.1021/acs.jproteome.5b01081
J. Proteome Res. 2016, 15, 2924−2934

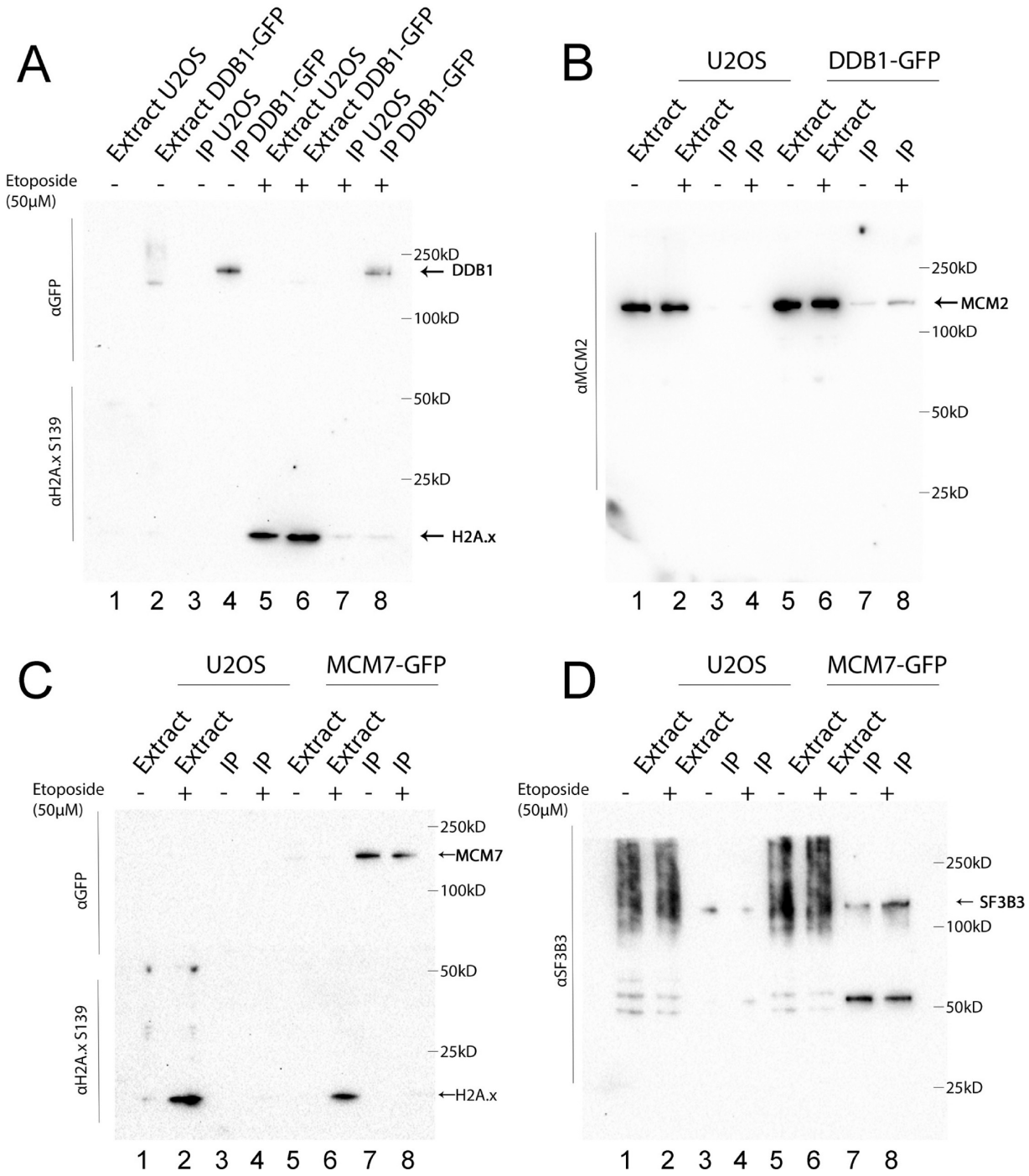

Figure 8. (A) U2OS cells expressing DDB1-GFP were mock-treated (lane 1−4) or treated with etoposide at 50 μM for 1 h. Cells were then washed and allowed to recover for 1 h (lane 5−8). Total cell extracts (lanes 1−2, 5−6) or immunoprecipitations with GFP-Trap agarose beads (IP, lanes 3−4, 7−8) were immunoblotted with GFP (top) or H2A.x phosphorylated on serine 139 (bottom) antibodies. (B) DDB1-GFP expressing U2OS cells were either untreated (lane 1, 3, 5, 7) or treated with etoposide at 50 μM for 1 h, washed, and allowed to incubate for 1 h (lane 2, 4, 6, 8). Cell extracts (lanes 1−2, 5−6) or cell extracts immunoprecipitated with GFP-Trap agarose beads (IP, lanes 3−4, 7−8) were immunoblotted with MCM2. (C) U2OS cells expressing MCM7-GFP were either mock-treated (lane 1, 3, 5, 7) or treated with etoposide at 50 μM for 1 h and allowed to recover for either 1 h (lane 2, 4, 6, 8). Total cell extracts (lanes 1−2, 5−6) or cell extracts immunoprecipitated with GFP-antibodies (IP, lanes 3−4, 7−8) were immunoblotted with GFP (top) or H2A.x phosphorylated on serine 139 (bottom) antibodies. (D) Cells expressing MCM7-GFP (lane 1, 3, 5, 7) or cells expressing MCM7-GFP treated with etoposide at 50 μM for 1 h washed and incubated for 1 h (lane 2, 4, 6, 8). Total cell extracts (lanes 1−2, 5−6) or cell extracts immunoprecipitated with GFP-Trap agarose beads (IP, lanes 3−4, 7−8) were immunoblotted with SF3B3.

proteins showing the highest confidence in the identification. As such, only the proteins showing a SILAC ratio enrichment over the control and identified were kept. Moreover, only proteins that were identified as interacting with at least two MCM proteins were retained during the analysis. The complete list of interacting proteins is available as Supplementary Tables, containing 418 proteins identified by immunoprecipitation of GFP-MCM proteins and 508 proteins identified by biotinylation of BirA-MCM proteins when comparing with proteins showing a SILAC ratio enrichment over the control. The number of

DOI: 10.1021/acs.jproteome.5b01081
J. Proteome Res. 2016, 15, 2924−2934

proteins overlapping in both type of experiments is thus much greater (Figure 5C) and represents 171 different proteins identified as interacting with the MCM complex and included several proteins previously reported. However, the number of false-positives is also most certainly higher, making the interpretation of new functions associated with the MCM complex less significant. Moreover, both methods are complementary as they do not identify necessarily the same proteins. AP−MS is more likely to identify proteins within the same complex, either through direct or indirect interactions with the bait protein, whereas PP−MS will identify proteins in the vicinity of the bait protein and will thus identify proteins that do not necessarily interact with or are part of the same complex as the bait protein. Nonetheless, the identification of these proteins is still informative to determine the context in which the protein of interest is under different conditions.

The identification of proteins interacting with the MCM complex following the treatment with DNA damage adds a level of complexity that allowed us to identify proteins involved in DNA repair. Among those proteins, we identified the DDB1-CUL4 complex, which is an ubiquitin-ligase complex involved in nucleotide excision repair. We had previously identified several ubiquitination sites distributed on several proteins of the MCM complex (MCM2, MCM3, MCM4, and MCM7).[26] Among those ubiquitination sites, several were significantly increased in response to DNA damage, suggesting a possible regulatory mechanism. These modifications were identified on all four MCM proteins, when only one exogenously expressed MCM protein was expressed, indicating that the modification is present on the endogenous MCM proteins as well and not resulting from the exogenous expression of the proteins.

Gene ontology annotations enrichment for biological processes identified two proteins involved in DNA repair (Figure 6B), namely, the topoisomerase II and the double-stranded RNA-dependent protein kinase (PKR). Recent studies demonstrated that PKR is involved in the cell response to genotoxic stress, and the PKR-knocked-out mouse embryonic fibroblasts (PKR−/−) are hypersensitive to bulky adduct DNA damage caused by UV radiation and cisplatin.[33] Interestingly, PKR localizes to the nucleus rapidly following these treatments, and this activity is required for resistance to cisplatin and the regulation of the cellular response to these DNA damaging agents. The DNA-damage-dependent interaction with the MCM complex suggests that PKR could be involved in regulating its function, possibly through the phosphorylation of MCM proteins.[26]

Additionally, the identification of proteins involved in ribosome biogenesis appeared intriguing at first, particularly considering that those proteins are very abundant and commonly found as contaminants in proteomics experiments. However, most of the proteins identified are part the NOP56/58 complex, which is involved in the assembly of the 60S ribosomal subunit and pre-rRNA processing, suggesting that the identification is most likely not due to contamination of abundant proteins in the extract. Interestingly, several components of the DNA replication initiation machinery and replication complex have been purified from nucleoli in human cells[34,35] and were shown in yeast to be associated with proteins involved in ribosome biogenesis,[36] further demonstrating a possible functional interaction between the MCM complex and ribosome biogenesis. Another protein function that was found to be associated with the MCM complex includes proteins involved in RNA processing, in particular, with SF3B proteins, which form the U2 small nuclear ribonucleoproteins complex (U2 snRNP) involved in mRNA splicing. As shown in Figure 7, several interactions between these proteins and proteins involved in DNA repair and cell cycle regulation have already been characterized, including CDC5L. Interestingly, the interaction between the MCM complex and SF3B was recently reported to be involved in RNA splicing of the epidermal growth factor receptor c-met.[37] Our data further confirm this observation and demonstrate that DNA damage may results in an increase in the interaction and thus affect splicing of different mRNA in response to DNA damage.

■ CONCLUSIONS

Using a quantitative approach with two different methods, we have mapped the interactomes of all components of the MCM complex. Although this study has identified a large number of putative protein interactions, we acknowledge that some proteins are likely to have been missed by our approach and that some of the proteins identified are possibly false-positive interactions. Importantly, we have confirmed in our study the identification of several proteins involved in DNA repair and cell cycle regulation, further confirming a role for the MCM complex in these mechanisms. Thus, the MCM complex appears to be playing multiple roles beyond DNA replication, which will be crucial to fully understand considering the recent interest in targeting this complex to treat human malignancies.

■ ASSOCIATED CONTENT

Supporting Information

The Supporting Information is available free of charge on the ACS Publications website at DOI: 10.1021/acs.jproteome.5b01081.

Supplementary Table captions. (PDF)

Supplementary Table 1: Table with data for AP−MS of MCM proteins. (XLSX)

Supplementary Table 2: Table with data for PP−MS of MCM proteins. (XLSX)

Supplementary Table 3: Table including the data presented in Figure 5. (XLSX)

Supplementary Table 5: Table summarizing the proteins whose interaction with the MCM complex is increased in response to DNA damage. (XLSX)

Supplementary Table 4: Table with the data presented in Figure 6. (XLSX)

■ AUTHOR INFORMATION

Corresponding Author

*Phone: 819-821-8000, ext. 75430. Fax: 819-820-6831. E-mail: fm.boisvert@usherbrooke.ca.

Notes

The authors declare no competing financial interest.

The mass spectrometry data have been deposited to the ProteomeXchange Consortium (http://proteomecentral.proteomexchange.org) via the PRIDE partner repository with the data set identifier PXD004089.

■ ACKNOWLEDGMENTS

M.-L.D. has a studentship from the Fonds de recherché Santé du Québec. Funding to FMB is from the Canadian Institutes of Health Research (MOP-123469) and from the National Sciences and Engineering Research Council of Canada (418404-2012).

DOI: 10.1021/acs.jproteome.5b01081
J. Proteome Res. 2016, 15, 2924−2934

REFERENCES

(1) Trinkle-Mulcahy, L.; Boulon, S.; Lam, Y. W.; Urcia, R.; Boisvert, F. M.; Vandermoere, F.; Morrice, N. A.; Swift, S.; Rothbauer, U.; Leonhardt, H.; Lamond, A. Identifying specific protein interaction partners using quantitative mass spectrometry and bead proteomes. *J. Cell Biol.* **2008**, *183*, 223−39.

(2) Vermeulen, M.; Hubner, N. C.; Mann, M. High confidence determination of specific protein-protein interactions using quantitative mass spectrometry. *Curr. Opin. Biotechnol.* **2008**, *19*, 331−7.

(3) Wang, X.; Huang, L. Identifying dynamic interactors of protein complexes by quantitative mass spectrometry. *Mol. Cell. Proteomics* **2007**, *7*, 46−57.

(4) Mellacheruvu, D.; Wright, Z.; Couzens, A. L.; Lambert, J. P.; St-Denis, N. A.; Li, T.; Miteva, Y. V.; Hauri, S.; Sardiu, M. E.; Low, T. Y.; Halim, V. A.; Bagshaw, R. D.; Hubner, N. C.; Al-Hakim, A.; Bouchard, A.; Faubert, D.; Fermin, D.; Dunham, W. H.; Goudreault, M.; Lin, Z. Y.; Badillo, B. G.; Pawson, T.; Durocher, D.; Coulombe, B.; Aebersold, R.; Superti-Furga, G.; Colinge, J.; Heck, A. J.; Choi, H.; Gstaiger, M.; Mohammed, S.; Cristea, I. M.; Bennett, K. L.; Washburn, M. P.; Raught, B.; Ewing, R. M.; Gingras, A. C.; Nesvizhskii, A. I. The CRAPome: a contaminant repository for affinity purification-mass spectrometry data. *Nat. Methods* **2013**, *10*, 730−6.

(5) Morris, J. H.; Knudsen, G. M.; Verschueren, E.; Johnson, J. R.; Cimermancic, P.; Greninger, A. L.; Pico, A. R. Affinity purification-mass spectrometry and network analysis to understand protein-protein interactions. *Nat. Protoc.* **2014**, *9*, 2539−54.

(6) Gingras, A. C.; Gstaiger, M.; Raught, B.; Aebersold, R. Analysis of protein complexes using mass spectrometry. *Nat. Rev. Mol. Cell Biol.* **2007**, *8*, 645−54.

(7) Roux, K. J.; Kim, D. I.; Raida, M.; Burke, B. A promiscuous biotin ligase fusion protein identifies proximal and interacting proteins in mammalian cells. *J. Cell Biol.* **2012**, *196*, 801−10.

(8) Lam, S. S.; Martell, J. D.; Kamer, K. J.; Deerinck, T. J.; Ellisman, M. H.; Mootha, V. K.; Ting, A. Y. Directed evolution of APEX2 for electron microscopy and proximity labeling. *Nat. Methods* **2014**, *12*, 51−4.

(9) Roux, K. J. Marked by association: techniques for proximity-dependent labeling of proteins in eukaryotic cells. *Cell. Mol. Life Sci.* **2013**, *70*, 3657−64.

(10) Weaver, L. H.; Kwon, K.; Beckett, D.; Matthews, B. W. Corepressor-induced organization and assembly of the biotin repressor: a model for allosteric activation of a transcriptional regulator. *Proc. Natl. Acad. Sci. U. S. A.* **2001**, *98*, 6045−50.

(11) Blow, J. J.; Gillespie, P. J. Replication licensing and cancer–a fatal entanglement? *Nat. Rev. Cancer* **2008**, *8*, 799−806.

(12) Blow, J. J.; Dutta, A. Preventing re-replication of chromosomal DNA. *Nat. Rev. Mol. Cell Biol.* **2005**, *6*, 476−86.

(13) Allen, C.; Ashley, A. K.; Hromas, R.; Nickoloff, J. A. More forks on the road to replication stress recovery. *J. Mol. Cell Biol.* **2011**, *3*, 4−12.

(14) Nam, E. A.; Cortez, D. ATR signalling: more than meeting at the fork. *Biochem. J.* **2011**, *436*, 527−36.

(15) Bell, S. D.; Botchan, M. R. The minichromosome maintenance replicative helicase. *Cold Spring Harbor Perspect. Biol.* **2013**, *5*, a012807.

(16) Sclafani, R. A.; Fletcher, R. J.; Chen, X. S. Two heads are better than one: regulation of DNA replication by hexameric helicases. *Genes Dev.* **2004**, *18*, 2039−45.

(17) Bochman, M. L.; Schwacha, A. The Mcm complex: unwinding the mechanism of a replicative helicase. *Microbiol Mol. Biol. Rev.* **2009**, *73*, 652−83.

(18) Arias, E. E.; Walter, J. C. Strength in numbers: preventing rereplication via multiple mechanisms in eukaryotic cells. *Genes Dev.* **2007**, *21*, 497−518.

(19) Bailis, J. M.; Forsburg, S. L. MCM proteins: DNA damage, mutagenesis and repair. *Curr. Opin. Genet. Dev.* **2004**, *14*, 17−21.

(20) Forsburg, S. L. Eukaryotic MCM proteins: beyond replication initiation. *Microbiol Mol. Biol. Rev.* **2004**, *68*, 109−31.

(21) Crevel, I.; Crevel, G.; Gostan, T.; de Renty, C.; Coulon, V.; Cotterill, S. Decreased MCM2−6 in Drosophila S2 cells does not generate significant DNA damage or cause a marked increase in sensitivity to replication interference. *PLoS One* **2011**, *6*, e27101.

(22) Crevel, G.; Hashimoto, R.; Vass, S.; Sherkow, J.; Yamaguchi, M.; Heck, M. M.; Cotterill, S. Differential requirements for MCM proteins in DNA replication in Drosophila S2 cells. *PLoS One* **2007**, *2*, e833.

(23) Lei, M.; Kawasaki, Y.; Tye, B. K. Physical interactions among Mcm proteins and effects of Mcm dosage on DNA replication in Saccharomyces cerevisiae. *Mol. Cell. Biol.* **1996**, *16*, 5081−90.

(24) Oehlmann, M.; Score, A. J.; Blow, J. J. The role of Cdc6 in ensuring complete genome licensing and S phase checkpoint activation. *J. Cell Biol.* **2004**, *165*, 181−90.

(25) Ibarra, A.; Schwob, E.; Mendez, J. Excess MCM proteins protect human cells from replicative stress by licensing backup origins of replication. *Proc. Natl. Acad. Sci. U. S. A.* **2008**, *105*, 8956−61.

(26) Drissi, R.; Dubois, M. L.; Douziech, M.; Boisvert, F. M. Quantitative Proteomics Reveals Dynamic Interactions of the Minichromosome Maintenance Complex (MCM) in the Cellular Response to Etoposide Induced DNA Damage. *Mol. Cell. Proteomics* **2015**, *14*, 2002−13.

(27) Cox, J.; Mann, M. MaxQuant enables high peptide identification rates, individualized p.p.b.-range mass accuracies and proteome-wide protein quantification. *Nat. Biotechnol.* **2008**, *26*, 1367−72.

(28) Cox, J.; Matic, I.; Hilger, M.; Nagaraj, N.; Selbach, M.; Olsen, J. V.; Mann, M. A practical guide to the MaxQuant computational platform for SILAC-based quantitative proteomics. *Nat. Protoc.* **2009**, *4*, 698−705.

(29) Trinkle-Mulcahy, L. Resolving protein interactions and complexes by affinity purification followed by label-based quantitative mass spectrometry. *Proteomics* **2012**, *12*, 1623−38.

(30) Kerrien, S.; Aranda, B.; Breuza, L.; Bridge, A.; Broackes-Carter, F.; Chen, C.; Duesbury, M.; Dumousseau, M.; Feuermann, M.; Hinz, U.; Jandrasits, C.; Jimenez, R. C.; Khadake, J.; Mahadevan, U.; Masson, P.; Pedruzzi, I.; Pfeiffenberger, E.; Porras, P.; Raghunath, A.; Roechert, B.; Orchard, S.; Hermjakob, H. The IntAct molecular interaction database in 2012. *Nucleic Acids Res.* **2012**, *40*, D841−6.

(31) Huang, D. W.; Sherman, B. T.; Lempicki, R. A. Systematic and integrative analysis of large gene lists using DAVID bioinformatics resources. *Nat. Protoc.* **2008**, *4*, 44−57.

(32) Huang, D. W.; Sherman, B. T.; Lempicki, R. A. Bioinformatics enrichment tools: paths toward the comprehensive functional analysis of large gene lists. *Nucleic Acids Res.* **2009**, *37*, 1−13.

(33) Bergeron, J.; Benlimame, N.; Zeng-Rong, N.; Xiao, D.; Scrivens, P. J.; Koromilas, A. E.; Alaoui-Jamali, M. A. Identification of the interferon-inducible double-stranded RNA-dependent protein kinase as a regulator of cellular response to bulky adducts. *Cancer Res.* **2000**, *60*, 6800−4.

(34) Ahmad, Y.; Boisvert, F. M.; Gregor, P.; Cobley, A.; Lamond, A. I. NOPdb: Nucleolar Proteome Database−2008 update. *Nucleic Acids Res.* **2009**, *37*, D181−4.

(35) Coute, Y.; Burgess, J. A.; Diaz, J. J.; Chichester, C.; Lisacek, F.; Greco, A.; Sanchez, J. C. Deciphering the human nucleolar proteome. *Mass Spectrom. Rev.* **2006**, *25*, 215−34.

(36) Zhang, Y.; Yu, Z.; Fu, X.; Liang, C. Noc3p, a bHLH protein, plays an integral role in the initiation of DNA replication in budding yeast. *Cell* **2002**, *109*, 849−60.

(37) Chen, Z. H.; Yu, Y. P.; Michalopoulos, G.; Nelson, J.; Luo, J. H. The DNA replication licensing factor miniature chromosome maintenance 7 is essential for RNA splicing of epidermal growth factor receptor, c-Met, and platelet-derived growth factor receptor. *J. Biol. Chem.* **2015**, *290*, 1404−11.

DOI: 10.1021/acs.jproteome.5b01081
J. Proteome Res. 2016, 15, 2924−2934